Advanced Composite Materials
Publication details, including instructions for authors and subscription information:
http://www.tandfonline.com/loi/tacm20

Degradation in Tensile Properties with Overlapped and Discontinuous Fabric Preforms

Thanh Trung Do [a] & Dong Joo Lee [b]
[a] Department of Mechanical Engineering, University of Technical Education HoChiMinh City, Vietnam
[b] School of Mechanical Engineering, Yeungnam University, Korea;, Email: djlee@yu.ac.kr
Version of record first published: 02 Apr 2012.

To cite this article: Thanh Trung Do & Dong Joo Lee (2011): Degradation in Tensile Properties with Overlapped and Discontinuous Fabric Preforms, Advanced Composite Materials, 20:5, 443-462

To link to this article: http://dx.doi.org/10.1163/092430411X576765

VSP

Advanced Composite Materials 20 (2011) 443–462

ADVANCED COMPOSITE MATERIALS
brill.nl/acm

Degradation in Tensile Properties with Overlapped and Discontinuous Fabric Preforms

Thanh Trung Do [a] **and Dong Joo Lee** [b,*]

[a] Department of Mechanical Engineering, University of Technical Education HoChiMinh City, Vietnam

[b] School of Mechanical Engineering, Yeungnam University, Korea

Received 5 August 2010; accepted 18 March 2011

Abstract

Measured tensile properties including the modulus, strength and elongation of resin transfer molded composites, which were fabricated using several fabric preforms through the normal, overlapped and discontinuous models, were compared. As expected, the overlapped and discontinuous models had lower tensile modulus and strength than the normal model; these values were functions of the effective fiber-volume fraction. The differences were examined and used to predict the overlap-damage and discontinuous-damage parameters, which were developed from the energy method, rule of mixture and failure modes. Also, the results showed that the final failures of the overlapped and discontinuous models were either interfacial bond failure or breaking fibers depending on the overlapped and discontinuous lengths. Since discontinuous fabrics in the preform cannot be avoided in designing and manufacturing composites, the ratio of the discontinuous gap to the gauge length (L_G/L) should be less than 0.05. Also, the ratio of the discontinuous length to the gauge length (L_D/L) should be large to minimize the influence of the stress concentration. Also, in light of the fiber-volume fraction, composites designed with the overlapped preform are better than those with the discontinuous preform.

Keywords

Resin transfer molding composites (RTMCs), overlaps, discontinuities, mechanical properties, failure mechanisms

1. Introduction

Resin transfer molded composites (RTMCs) have been used in a number of notable illustrative applications; extensive literature exists on their mechanical properties and costs that permits comparisons with other traditional methods of fabrication [1–3]. However, some unavoidable problems pertaining to the void content [4, 5], stacking sequence [6, 7] and geometrical preform configurations [8, 9], and in par-

* To whom correspondence should be addressed. E-mail: djlee@yu.ac.kr
Edited by the KSCM

DOI:10.1163/092430411X576765

ticular, overlapped and discontinuous fabric preform patterns, can occur during the preform loading, injection and/or curing processes due to the complexity of the shape. These problems can cause considerable scatter in the stress concentration and initial cracks. Also, failure initiation as a consequence of the shear factors and stress transfer varies for different preform models in terms of the number and lengths of overlaps and discontinuities. It is believed that the presence of those defects tends to degrade the quality of composites as a function of the effective fiber-volume fraction.

Steenkamer *et al.* [8] studied the influence of preform joints on the processing of resin transfer molded composites for different joint configurations. The joints help to form large composite parts of complex shapes, such as the front structure of automobile and automotive cross-members. The computational and experimental results showed that the permeability of the preform was remarkably different near the joint. When the resin first hits the joint region, a pressure gradient does not exist to drive the fluid down the length of the joint towards the side walls of the mold, which may cause unregulated flow and even failure to fill the mold successfully. Holmberg and Berglund [10] also studied the problems of the fiber preforms of U-beams and tensile failure mechanisms. They observed that the reinforcement easily led to fabric discontinuity in the preform during preforming and/or mold closure. This phenomenon caused problems of void content and crack initiation in the finished composites. However, the use of composites with discontinuous fibers has increased due to many advantages regarding cost-effective, thermodynamic properties and processing techniques as well as the demands of both local and global loading conditions.

Also, several authors have studied the damage and failure mechanisms of discontinuous fiber composites [11–14]. Damage to composites involves several types of local degradation processes, such as matrix micro-cracking, interfacial debonding, fiber pull-out and fiber breakage. They can occur simultaneously and thus reduce the overall mechanical properties. For discontinuous fibers, due to the efficiency of the load transfer, stress transfer and stress concentrations at the fiber ends, the shear factors and interfacial degradation serve to degrade the quality of composites. Lee *et al.* [15] presented the joint strengths, peel stresses and failure modes in an adhesively bonded double-strap and supported single-lap glass fiber-reinforced polymer joints. The tensile strength and failure mechanisms of their specimens depended on not only the stiffness values of the materials but also the adhesive length. The joint strength increased as the adhesive length continued to increase, and the peeling effect was crucial to the failure behavior of the adhesively bonded joints. Jain and Mai [16] analyzed and examined the failure strength on the basis of the failure modes for resin-transfer-molded single-lap joints. They concluded that the moment factor due to the lap joint was one of the main factors that created failure at the interface between the two adhesive layers. The influence of the material and structure of composites on the shear strength was considered as well. Hence, further research is necessary to enhance an understanding of the influence of discontinuous fabric

preform configurations on the mechanical properties and failure mechanisms of the respective composites.

The objective of this study is to examine various structural influences that several overlapped and discontinuous models with different effective fiber-volume fractions have on the tensile properties. On the basis of an energy method, a simple analysis for the tensile modulus is also performed. The results are compared with experimental data for considering the influence of overlapped and discontinuous patterns using the overlap-damage and discontinuous-damage parameters. Also, the shear strengths and failure modes due to overlaps and discontinuities are determined as functions of the preform type and fabric layers. In addition, the tensile modulus and strength of the overlapped and discontinuous models are compared with the results of the normal model to help clarify the influence of fabric preform configurations.

2. Experimental

The initially laminated composites were made from the resin transfer molding method with several preform models, including normal, overlapped and discontinuous, and various effective fiber-volume fractions. The details of the geometrical fabric preform types are as follows (see Fig. 1).

- Model 1 is a normal type. The fabric preform has varying numbers of plane fabric layers, i.e., 2, 4, 6, 8 and 10.
- Models O-1, O-2 and O-3 are the overlapped fabric preform patterns with varying numbers of fabric layers, *viz.*, 2, 4 and 8 layers, respectively.
- Models D-1, D-2 and D-3 are the discontinuous fabric preform patterns. The numbers of discontinuous fabric layers are 2, 4 and 6 for Models D-1, D-2 and D-3, respectively. In the configurations of those models, the gap at discontinuous locations is extremely small and assumed to be zero ($L_G = 0$). The region between two discontinuous locations is called the discontinuous section or discontinuous length (L_D).

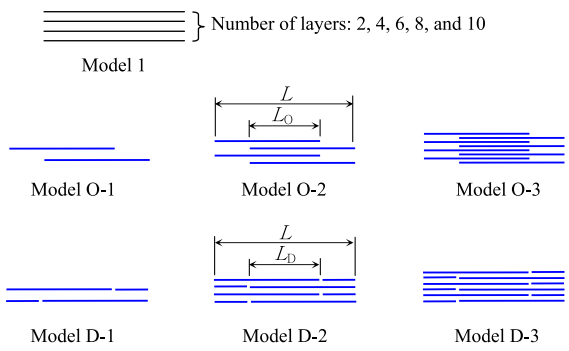

Figure 1. Geometrical fabric preform configurations. This figure is published in color in the online version.

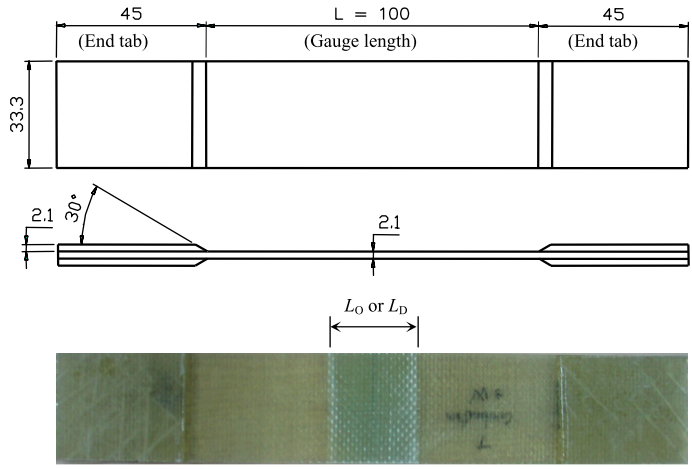

Figure 2. Specimen for the tensile test. This figure is published in color in the online version.

The materials prepared for making the laminated composites were polyester resin R235 (density of $\rho = 1.05$ g/cm^3, tensile modulus of $E = 1.3$ GPa and tensile strength of $\sigma_{max} = 36$ MPa) from Sewon Chemical Co. and E-glass woven fabric K618 ($\rho = 2.54$ g/cm^3, $E = 70$ GPa and $\sigma_{max} = 3.4$ GPa) from Hankuk Fibers Co. In order to reduce the curing time, the hardener material of Luperox DDM from Seki Arkema Co. was mixed with the resin in a ratio of 1:120 by weight.

The test specimens were cut by an electric band-saw from an original plate of size 300 mm × 200 mm. The dimensional specimens were modeled in accordance with the ASTM D3039-76 standard tensile test with a gauge length of $L = 100$ mm and a rectangular cross-section of thickness, $t = 2.1$ mm, and width, $b = 33.3$ mm. Also, the ends of the specimens were adhesively bonded by laminated tabs for load transfer from the machine grips to the specimens without damage to the specimens, as shown in Fig. 2. All the tests were done by using a Shimazu testing machine at room temperature and a relative humidity of 50%. First, two end-tabs of each specimen were clamped in the grips of the tensile testing machine. Then, the tensile load was applied with a test speed of 3 mm/min.

Typically, the ratios of the overlapped length to the gauge length (L_O/L) and the discontinuous length to the gauge length (L_D/L) were varied from 0.05 to 0.9. At least three specimens were examined for each sample group from which the mean values were reported.

3. Results and Discussion

3.1. Tensile Strength and Failure Mechanisms

The tensile strength of the composites with different fabric preform configurations was determined from the maximum load (P_{max}) and the original cross-sectional area (A) of the respective specimens [17, 18]. The fiber-volume fraction was cal-

culated using the densities of the matrix, fiber and composite [17, 19]. In this examination, the plain woven fabric K618 had the 'fiber' symmetry as in woven or cross-plied as 0° and 90° fiber reinforcement. Also, the load was applied as the 0° direction for cases of the overlapped and discontinuous specimens. Thus, the effective fiber-volume fraction (V_f) as the load carrying fibers were assumed to be only 50% of the fibers in the fabric perform for better comparison. As shown in Fig. 3(a) and (b), the tensile strength of the overlapped and discontinuous models exhibited two regimes as functions of L_O/L and L_D/L, respectively, depending on both the effective fiber-volume fraction (through the number of layers) and the geometrical preform type (through the shear strength). Since the tensile load always increased with the axial elongation up to final failure with a loud 'bang' sound, the tensile strength was considered as the failure strength, which depended on the failure load, failure location, and failure modes under tensile loading [15, 16]. The damage to a composite with a preform deformation involved several types of local degradation processes, such as matrix micro-cracking, fiber pulling and fiber breaking that served to reduce the overall mechanical properties of the respective composites [7, 10, 20].

For the first regime (I), where the overlapped and discontinuous lengths were smaller than the critical overlapped and discontinuous lengths, i.e., $L_O < L_{CO}$ and $L_D < L_{CD}$, respectively, failure occurred at the interfacial bonds of the overlapped and discontinuous sections of the composites. The interfacial bond failed before the fibers could achieve their potential strength, which related to not only the material stiffness but also the adhesive length [18, 20, 21]. As shown in Fig. 4(a) and (c), the experimental results showed that the failure mechanisms of both the overlapped and discontinuous models were pulling failure as in Mode II, which was crucial to the failure behavior of adhesively bonded overlaps and discontinuities within this regime's boundary condition. The shear factor and interfacial bonding degradation due to the geometrical structural deformations served to degrade the tensile strength of the respective composites. The failure mechanisms can also be analyzed as follows.

For the overlapped models, consider an infinitesimal length, dL_O, which belongs to L_O, as shown in Fig. 5(a). The most common functions of the matrix are to provide a means of distributing the load among the fibers and transmitting the load between the fibers and to resist pulling failure. However, the tensile moduli and strengths of the matrix and fiber are different, and the longitudinal strain in the matrix is larger than that in the fiber due to the differential properties of the two materials. If a perfect bond is assumed for each fabric layer, the difference in the longitudinal strains creates a shear stress in the overlapped section, when $L_O < L_{CO}$.

The force equilibrium equations are:

$$bt_f(\sigma_f + d\sigma_f) - bt_f\sigma_f - 2b(dL_O)\tau_O = 0 \quad \text{and} \quad \frac{d\sigma_f}{dL_O} = \frac{2\tau_O}{t_f}. \tag{1}$$

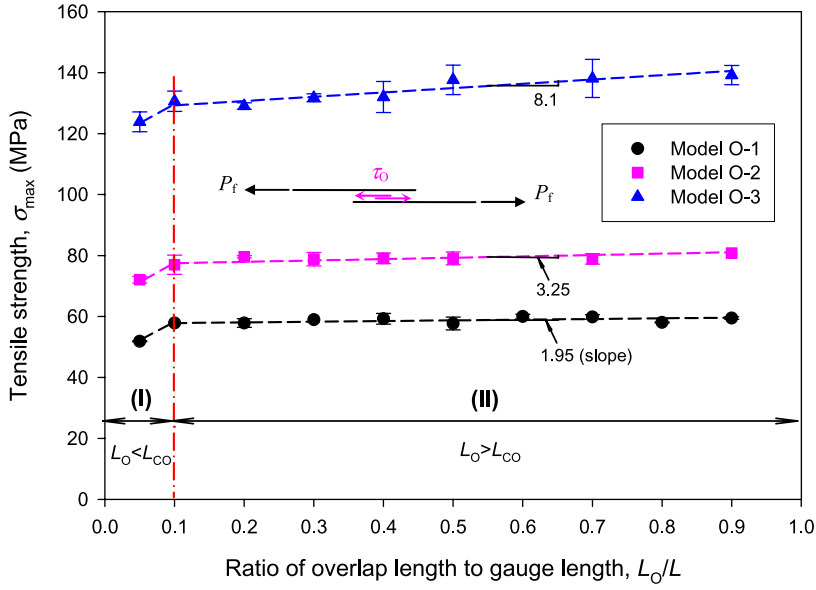

(a)

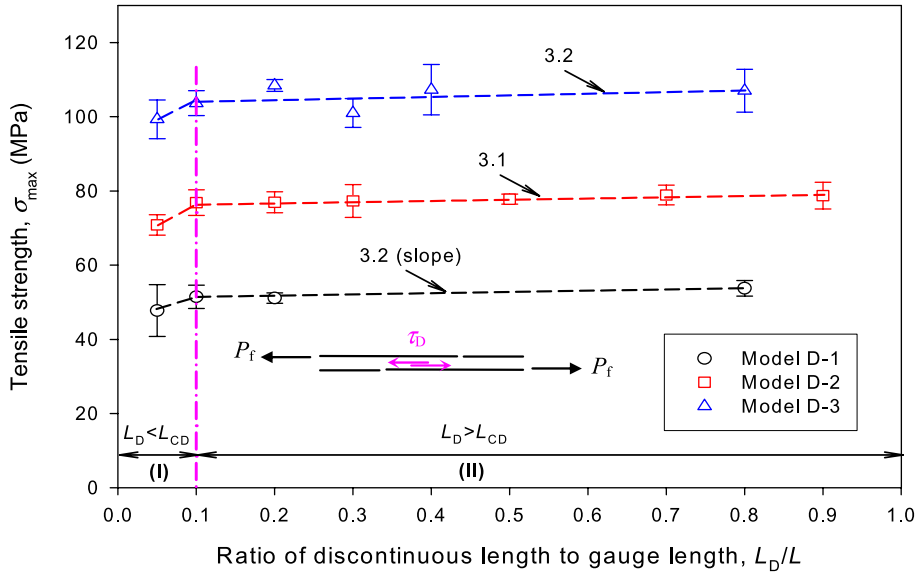

(b)

Figure 3. Variation of the tensile strength for: (a) overlaps and (b) discontinuities. This figure is published in color in the online version.

For simplicity of analysis, it is often assumed that the interfacial shear stress (τ_O) is a constant. Thus,

$$\sigma_f = \frac{2\tau_O}{t_f} L_O, \tag{2}$$

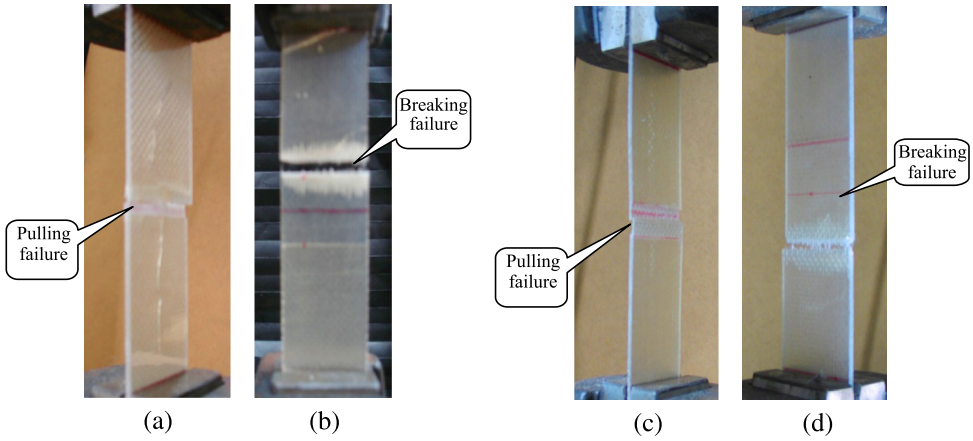

Figure 4. Failure mechanisms of composites with overlapped and discontinuous preforms. (a) Model O-2, $L_O/L = 0.05$. (b) Model O-2, $L_O/L = 0.2$. (c) Model D-1, $L_D/L = 0.05$. (d) Model D-3, $L_D/L = 0.3$. This figure is published in color in the online version.

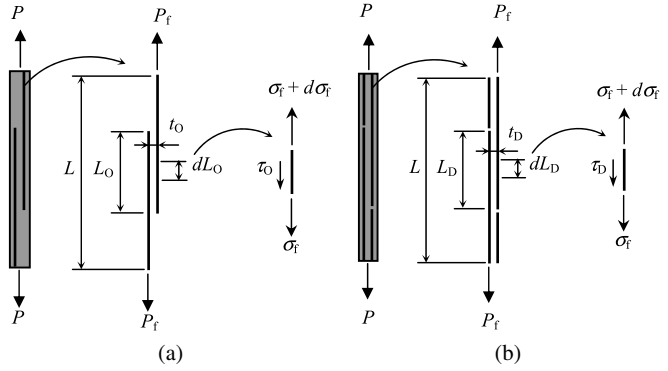

Figure 5. Models used in the analytical study.

where σ_f is the longitudinal stress of the fiber and t_f is the thickness of the layer.

When the laminated composite contains overlapping fabric layers that can be considered as being discontinuous fibers, the fiber stress is not uniform. It is zero at the ends of the overlapped section and linearly builds up to a maximum value at the central portion of the fiber [22]. The maximum fiber stress due to the shear factor that can be achieved at a given load is:

$$(\sigma_f)_{max} = \frac{2\tau_O}{t_f}\frac{L_O}{2} = \frac{\tau_O}{t_f}L_O. \tag{3}$$

Based on the rule of mixture, the tensile strength of the composite with an overlapped fabric preform for a boundary condition of $L_O < L_{CO}$ can be given by:

$$\sigma_{max} = \left(\frac{\tau_O}{t_f}L_O\right)V_f + \sigma'_m(1 - V_f), \tag{4}$$

where V_f is the effective fiber-volume fraction and σ'_m is the matrix stress at the instant of composite failure that can be predicted based on the elongation. Then, the tensile strength of the overlapped models for regime (I) can be determined through equation (4).

Similarly, for the discontinuous model (see Fig. 5(b)), the failure was due also to Mode II owing to the pulling out of layers at the discontinuous section. Pulling failure occurred when the discontinuous length (L_D) was smaller than the critical discontinuous length (L_{CD}), as shown in Fig. 4(c). Thus, the tensile strength of the composite with the discontinuous fabric preform for a boundary condition of $L_D < L_{CD}$ can be calculated by:

$$\sigma_{max} = \left(\frac{\tau_D}{t_f} L_D\right) V_f + \sigma'_m(1 - V_f), \tag{5}$$

where τ_D is the interfacial shear strength of the discontinuous section.

As expected, the shear strength of composites with the overlapped and discontinuous models can be predicted from equations (4) and (5) for cases of failure behavior that are due to the interfacial bonding, which depends on the materials, effective fiber-volume fraction, bonding area and loading conditions.

For the second regime (II), where the overlapping length was larger than the critical overlapping length ($L_O > L_{CO}$) and the discontinuous length was larger than the critical discontinuous length ($L_D > L_{CD}$), the failure of the respective composites was due to breaking fibers without pulling failure, as shown in Fig. 4(b) and (d). The failure strength was mainly controlled by the potential strength of fibers. However, the stress concentrations at the ends of the overlapped and discontinuous sections as well as the degradation in load carrying due to the discontinuous fibers could be one of the main factors that created failure at the discontinuous locations of the fibers and served to degrade the quality of composites [10, 23, 24]. Also, owing to the overlapped and discontinuous configurations of the preform, the resin transfer molding process might have unregulated the permeability and even increased the void content [8]. Thus, for overlapping and discontinuous lengths within the boundary conditions of $L_O > L_{OC}$ and $L_D > L_{CD}$, the maximum fiber stress may reach the ultimate fiber strength (σ_{fu}); the tensile strength of the composites with overlapped and discontinuous fabric preforms are then given by:

$$\sigma_{max} = C_O \sigma_{fu} V_f + \sigma'_m(1 - V_f) \quad \text{and} \quad \sigma_{max} = C_D \sigma_{fu} V_f + \sigma'_m(1 - V_f). \tag{6}$$

In equation (6), C_O and C_D are 'damage' parameters for the tensile strength, which account for the weakening of the composite due to the overlapped and discontinuous patterns; these should be less than unity.

In general, a composite becomes much stronger and stiffer with increasing effective fiber-volume fraction as well as interfacial bonding area of the overlapped and discontinuous sections, which is related to the stacking sequence, load carriage, and shear factor [7, 25]. These are the reasons why the tensile strength was always increasing with the overlapping and discontinuous lengths for both regimes. The

experimental results showed that the critical overlapping and discontinuous lengths were the same, having a constant value with $L_{CO}/L = L_{CD}/L = 0.1$, regardless of the number of fabric layers. This was due to the sequence of the configuration in the preform and the nature of the materials. For the first regime, the failure type could be related to the tensile strength that was controlled by the interfacial bonding strength depending on the overlapping and discontinuous fabric lengths. For the other regime, the failure was controlled by the potential strength of the fabric when the overlapping and discontinuous lengths reached the critical values.

The shear strengths (τ_O and τ_D) were determined from equations (4) and (5), when $L_O = L_{CO}$ and $L_D = L_{CD}$, respectively, and are described in Table 1. Also, the shear stresses for certain overlapped and discontinuous lengths could be predicted from the given values of the properties of the matrix and fiber materials, effective fiber-volume fraction, and tensile load. The measured results showed that the shear strengths of the overlapped models were larger than those of the discontinuous models. Each type of preform had almost the same shear strength even when the number of fabric layers varied; for instance, the shear strength, τ_O, was approximately 19 MPa for the overlapped models (see Table 1). It is believed that the load-carrying capacity of the overlapped models was superior to that of the supported discontinuous preform type. And the shear strengths of the overlapped models were almost the same, independent of the fabric layer number in the preform. The shear strengths of the overlapped and discontinuous sections were smaller than the matrix strength, which provided a means of distributing the load among the fibers and transmitting the load between the fibers [26]. It can be concluded that the shear strength was decided by not only the interfacial bonding area but also the preform type [22, 27].

Figure 6 depicts a tensile strength comparison across the normal, overlapped, and discontinuous models *vs.* the effective fiber-volume fraction (V_f), which was in proportion to the overlapped and discontinuous lengths (see Fig. 7). Due to the typical configurations, the measured V_f rose with the overlapped length; however, it was a

Table 1.
Calculated shear strengths (τ_O and τ_D) derived from equations (4) and (5), at the critical overlapped length (L_{CO}) and the critical discontinuous length (L_{CD})

	Model	L_{CO} (mm)	V_f (%)	σ_c (MPa)	σ'_m(MPa)	τ_O (MPa)
Overlap	O-1	10	2.28	55.847	32	19.4
	O-2	10	4.56	79.554	33	19
	O-3	10	9.13	129.02	34.5	19.3
	Model	L_{CD} (mm)	V_f (%)	σ_c (MPa)	σ'_m(MPa)	τ_D (MPa)
Discontinuity	D-1	10	4.19	51.474	23.5	12.5
	D-2	10	8.37	76.858	24	11.9
	D-3	10	12.56	103.66	25	11.8

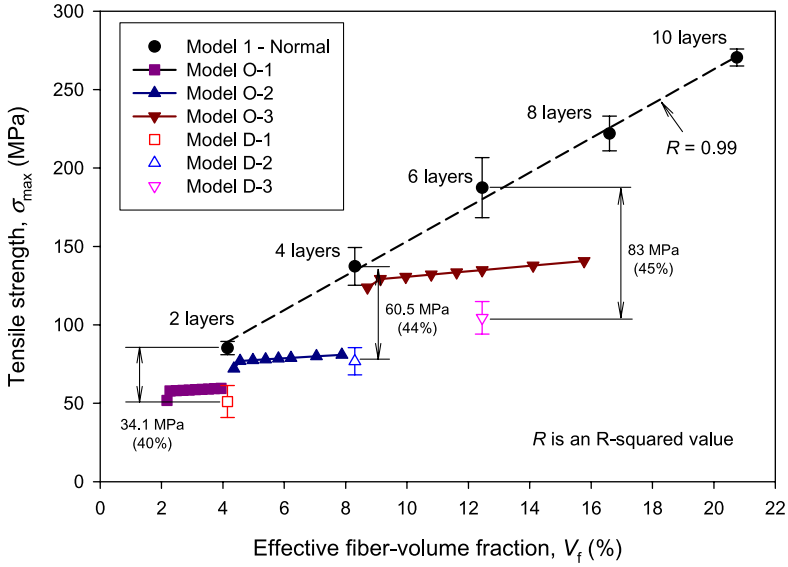

Figure 6. Tensile strength *vs.* V_f for the normal, overlapped and discontinuous models. This figure is published in color in the online version.

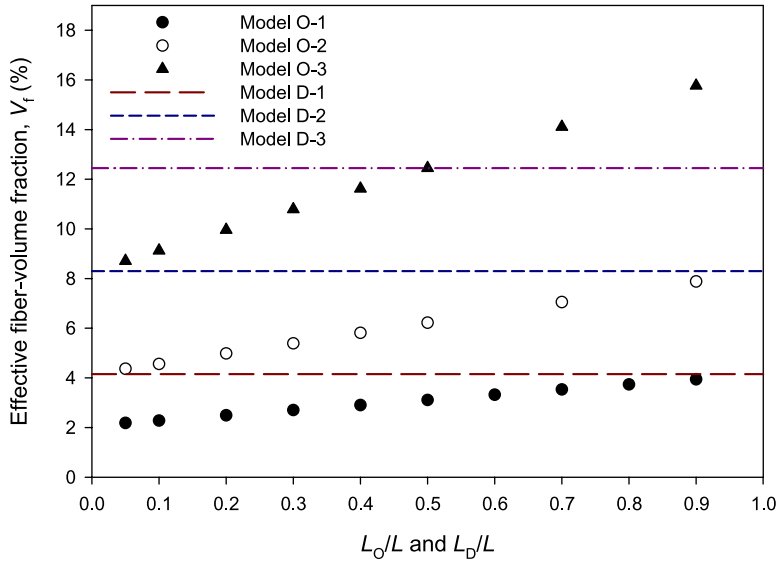

Figure 7. Effective fiber-volume fraction *vs.* the overlapping and discontinuous lengths. This figure is published in color in the online version.

constant value even when the discontinuous length varied in the preform. It can be seen that the experimentally measured results of the overlapped and discontinuous models were smaller than those of the normal model as a function of V_f. This was due to the influence of the discontinuous fibers with the contributions of the load and

stress transfers [18, 22, 28] existing at the ends of the overlapped and discontinuous sections. Also, those influences were much larger when the overlapped and discontinuous lengths as well as the number of fabric layers in the preform increased. For regime (I), the failure of composites occurred at the interfacial bonds [15, 17, 29] of the overlapped and discontinuous sections, which failed before the fibers achieved their respective potential strength. Thus, the lower strength of composites with discontinuous fibers during this regime was reasonable. For regime (II), due to the stress concentrations [17, 22–24], the composite failures occurred at the ends of the overlapped and discontinuous sections. While the failure of the composite with the normal preform always occurred at a mid-gauge length, the maximum fiber stress at the mid-gauge length could reach the ultimate fiber strength. In turn, this implied that as a function of V_f, the tensile strength of the overlapped and discontinuous models with a larger number of overlapped and discontinuous layers was much smaller than that of the normal model. For instance, the average strengths regarding lower values were about 34.1, 60.5 and 83 MPa for Models D-1, D-2 and D-3, respectively. Those values are quite low when compared with the normal models for the same number of fabric layers. In addition, the distribution and transfer of the load between fibers for the overlapped models was better than that for the discontinuous models, and the tensile strength of the overlapped models was larger than that of the discontinuous models as a function of the effective fiber-volume fraction.

Figure 8 depicts the overlap-damage and discontinuous-damage parameters in relation to the tensile strength (C_O and C_D) derived from equation (6) when $L_O > L_{CO}$ and $L_D > L_{CD}$. It can be seen that those values, C_O and C_D, were

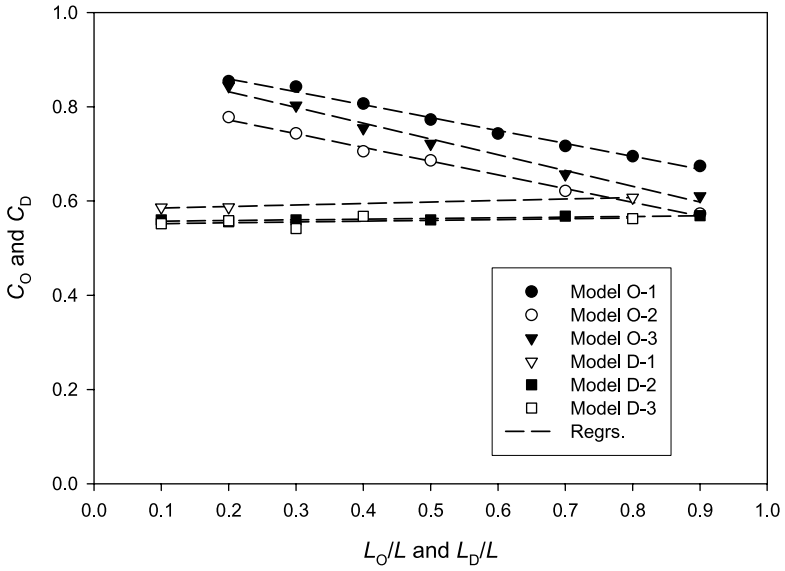

Figure 8. The overlap-damage and discontinuous-damage parameters corresponding to the tensile strength.

less than 1. This was due to the influence of discontinuous fibers in the composites, which caused the stress transfer and stress concentrations at the ends of the overlapped and discontinuous sections as well as the degradation in load carrying under tension. For the overlapped models, the overlap-damage parameter decreased with increasing overlapping length, in as Model O-1: $C_O = 0.85$, $C_O = 0.77$ and $C_O = 0.67$ when $L_O/L = 0.2$, $L_O/L = 0.5$ and $L_O/L = 0.9$, respectively. This meant that the fiber strengths of those composites were 85%, 77% and 67%, respectively, compared to the continuous fibers in the normal preform (Model 1), which was expected for a given effective fiber-volume fraction. It is clear that the influence of the overlapped models on the tensile strength was much larger when the overlapping length in the preform increased. However, the discontinuous models manifested a small difference in the damage-discontinuous parameters, specifically $0.55 < C_D < 0.6$, as a function of the discontinuous length within $L_{CD}/L < L_D/L < 1$. This implied that the influence of the discontinuous location on the tensile strength was almost the same for regime (II). Also, the influence of the overlapped and discontinuous fabric preforms on the tensile strength was the same when the ratios of both the overlapping length to the gauge length (L_O/L) and the discontinuous length to the gauge length (L_D/L) reached unity, regardless of the number of fabric layers. The reduction in strength was also caused by processing, which was related to the void content and stacking sequence, as well as the loading conditions [4, 8, 30]. In some cases, it can reduce the damage from the discontinuous fabric patterns to the mechanical properties through several extra continuous fabric layers in the preform to reduce the stress concentrations [10].

To verify the stress concentration factor due to the discontinuous fabrics, which affect the quality of composites, the tensile strength for Model D-2 was considered under several ratios of the discontinuous gap to the gauge length (L_G/L), as shown in Fig. 9. It can be seen that the tensile strength varied as the discontinuous gap increased, and had the highest value at $L_G/L = 0.05$, which was the critical value. It meant that the influence of the stress concentration decreased as L_G/L increased from 0 to 0.05. When $L_G/L > 0.05$, the stress concentration was negligible and the tensile strength was dominated by the potential strength of the fibers. It led to a decrease in the tensile strength with increasing L_G/L or decreasing effective fiber-volume fraction within $L_G/L > 0.05$. It can be concluded that the tensile strength of composites with a discontinuous preform was dependent on not only the effective-fiber volume fraction but also the discontinuous gap, which was related to the stress concentration that was one of the factors for controlling the tensile strength of composites. In general, the tensile strength can be calculated as follows.

When the discontinuous gap is smaller than the critical value, i.e., $L_G/L < L_{CG}/L$, the tensile strength is given by the relationship:

$$\sigma_{max} = k\left(\frac{L_G}{L}\right)^2 + q\left(\frac{L_G}{L}\right) + C_D\sigma_{fu}V_f + \sigma'_m(1 - V_f), \tag{7}$$

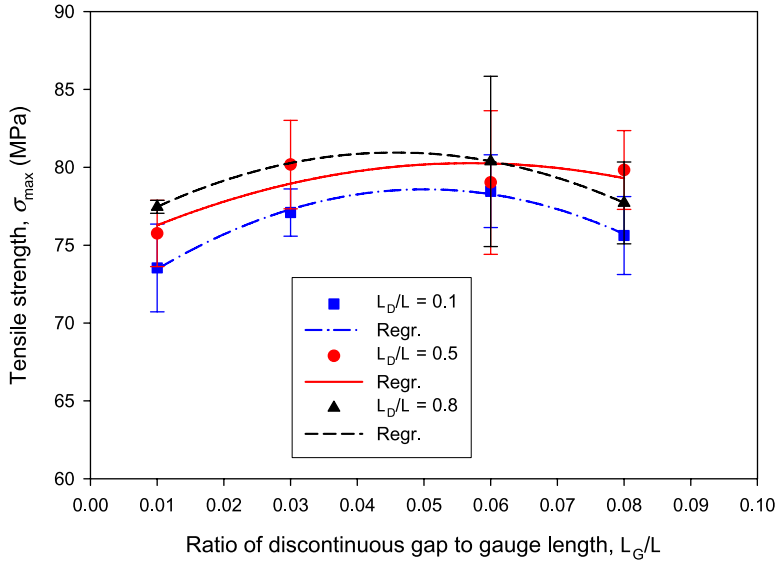

Figure 9. Tensile strength of the discontinuous model for different discontinuous gaps. This figure is published in color in the online version.

where both k and q are constants of the composite that depend on the matrix properties, specimen geometries, loading conditions, etc. In this study, it was found that $k = -1812$ and $q = 206$ for the discontinuous fabric preform deformation under a tensile test speed of 3 mm/min. Depending on the design and manufacturing conditions, it is possible to use the above relationship to predict the tensile properties of composite products.

If the discontinuous gap is larger than the critical value, i.e., if $L_G/L > L_{CG}/L$, the tensile strength is given by:

$$\sigma_{max} = C_D \sigma_{fu} V_f + \sigma'_m (1 - V_f). \tag{8}$$

3.2. Tensile Modulus and Elongation

Figure 10(a) and (b) depicts the tensile modulus of composites fabricated from the overlapped and discontinuous fabric preforms, respectively. The tensile modulus increased linearly with the overlapped length (see Fig. 10(a)) as well as the discontinuous length (see Fig. 10(b)), and had a larger slope with an increasing number of fabric layers in the preform. As expected, the composite with a higher fiber-volume fraction had a larger tensile modulus [19]. For the overlapped models, differences in the effective fiber-volume fraction led to different slopes in the tensile modulus of the respective composites as functions of L_O/L and the number of fabric layers. For the discontinuous models, the slope increased slightly when L_D/L increased from 0.05 to 0.9, and was almost the same for any number of fabric layers in the preform. For instance, the slope was 0.13 for Model D-2 and 0.14 for both Model D-1 and Model D-3. This implied that the influence of discontinuous location on the tensile

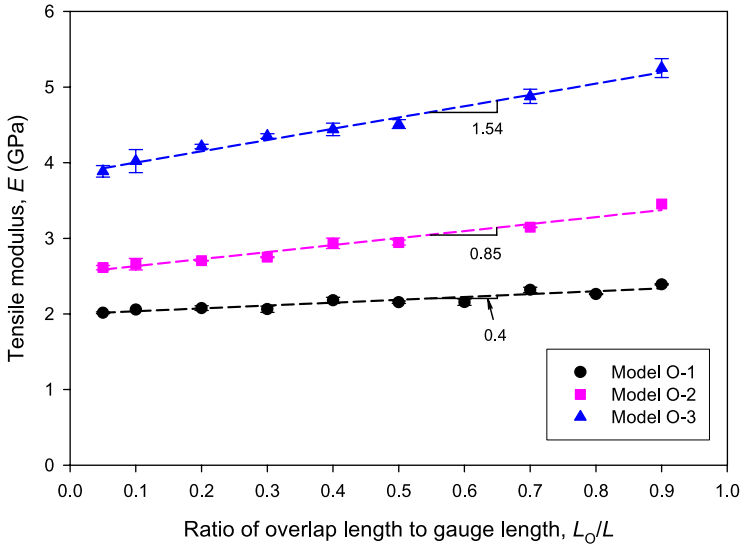

(a)

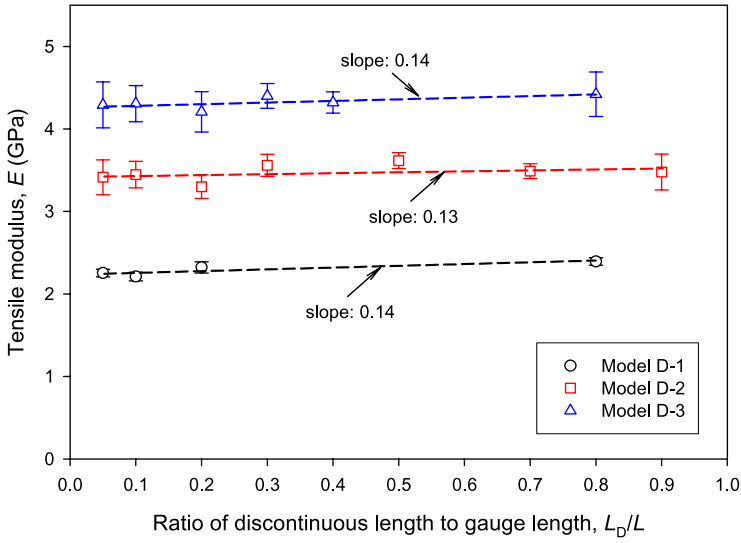

(b)

Figure 10. Tensile modulus of composites with fabric preform deformations: (a) overlaps and (b) discontinuities. This figure is published in color in the online version.

modulus was negligible in the range of $0 < L_D/L < 1$, regardless of the number of discontinuous fabric layers in the respective composite.

The variation of the tensile modulus of the normal, overlapped, and discontinuous models *vs.* the effective fiber-volume fraction is shown in Fig. 11. Load transfer and stress transfer occurred at the ends of the overlapped and discontinuous sections and the interfaces between neighboring fibers due to the influence of the discontinu-

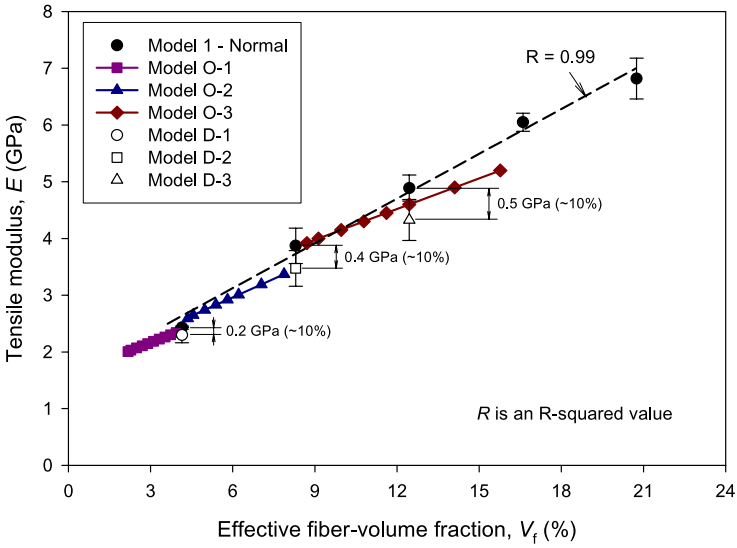

Figure 11. Variation of the tensile modulus with V_f for the normal, overlapped and discontinuous models. This figure is published in color in the online version.

ous fibers. As a result, the load-carrying capacity was degradable for the composites with discontinuous fibers. Also, the longitudinal strains of the overlapped and discontinuous sections were larger than the longitudinal strain of the normal section due to the influence of the shear factor [22, 25]. In other words, the tensile modulus of the overlapped and discontinuous models was probably smaller than that of the normal model for a given effective fiber-volume fraction. For instance, the average values of the lower tensile modulus were approximately 0.2, 0.4 and 0.5 GPa for Models D-1, D-2 and D-3, respectively, which compared well with the results for the normal model for the same effective fiber-volume fraction.

To facilitate an understanding of the influence of overlapped and discontinuous patterns, a simple analysis of the tensile modulus that is based on the energy method is performed as shown in the following equations:

$$\lambda = \frac{2U}{P} = \frac{P}{bt}\left[\frac{L - L_O}{E_1} + \frac{L_O}{E_2}\right] \quad \text{for the overlapped models,} \tag{9}$$

$$\lambda = \frac{2U}{P} = \frac{PL}{btE} \quad \text{for the discontinuous models.} \tag{10}$$

In equations (9) and (10), λ is the analytical elastic elongation, U is the elastic energy, P is the tensile load, b and t are the width and thickness of the specimen, respectively, E_1 and E_2 are the tensile moduli for the non-overlapped and overlapped sections, respectively, and E is the tensile modulus for the entire specimen assuming the gap at the discontinuous location is zero. Those tensile moduli can be predicted from the normal model (Model 1) with a given number of fabric layers.

Due to the influence of discontinuous fibers, the analytical elastic elongation, λ, differs from the experimental results (λ^*). The difference can be captured in the form, $\lambda^* = \beta\lambda$, for the overlapped models and in the form, $\lambda^* = \gamma\lambda$, for the discontinuous models. The values of β and γ are the overlap-damage and discontinuous-damage parameters, respectively, regarding the tensile modulus that arise from the degradation in load carrying.

We assume that those tensile moduli are constant values, which are predicted from the normal preform type (Model 1). E_1 is 2.1, 2.5 and 3.75 GPa for Models O-1, O-2 and O-3, respectively. E_2 is 2.5, 3.75 and 5.9 GPa for Models O-1, O-2 and O-3, respectively, and E is 2.5, 3.75 and 4.8 GPa for Models D-1, D-2 and D-3, respectively.

Figure 12 depicts the experimental and analytical results of the elastic elongation at $P = 2.01$ and $P = 1.5$ kN with increasing L_O/L and L_D/L, respectively, for various overlapped models (Fig. 12(a)) and discontinuous models (Fig. 12(b)). The values that predicted using equations (7) and (8) were in good agreement with $\beta = 1.03$ for the overlapped models and $\gamma = 1.11$ for the discontinuous models, regardless of the number of fabric layers in the preform. This meant that the influence of the 'damage' parameters on the tensile modulus depended only on the geometrical preform type, but did not vary with the effective fiber-volume fraction. The load transfer and stress transfer occurred with both the overlapped and discontinuous models, which related to load carrying and stress distribution in the respective composites. As a result, the elastic elongations of the composites with discontinuous fibers were larger than those of the composites with continuous fibers. In general, the 'damage' parameters, α and $\beta > 1$, clearly indicated that the overlapped and discontinuous patterns always affected the quality of the finished composites, in terms of not only the tensile modulus and strength but also the elastic elongation. Also, $\beta < \gamma$, which means the influence of the discontinuous models on the tensile modulus was larger than that of the overlapped models. In other words, the mechanical properties were more sensitive to the discontinuous preform deformation than was the case in the overlapped models.

To verify that the tensile properties of composites depended on not only the preform deformation but also the material properties, one more matrix, *viz.*, R409 ($E = 1.1$ GPa and $\sigma_{max} = 31$ MPa) from Sewon Chemical Co. was used for fabricating the composites, which was expected for the same fiber, i.e., K618, and processing conditions. Several extra preform types were preformed; these included the normal models with five, seven, and nine fabric layers and an overlapped model, say, Model O-E, having six fabric layers in the overlapped section with $L_O/L = 0.15, 0.3$ and 0.45. The standard tensile tests were also used with a gauge length of $L = 100$ mm, specimen thickness of $t = 2.5$ mm, and specimen width of $b = 33$ mm. The results showed that the tensile moduli of the K618/R409 composites also increased with the effective fiber-volume fraction for both the normal and overlapped models, as shown in Fig. 13. However, the results for composites with a low modulus matrix (R409) were much smaller than those for composites with

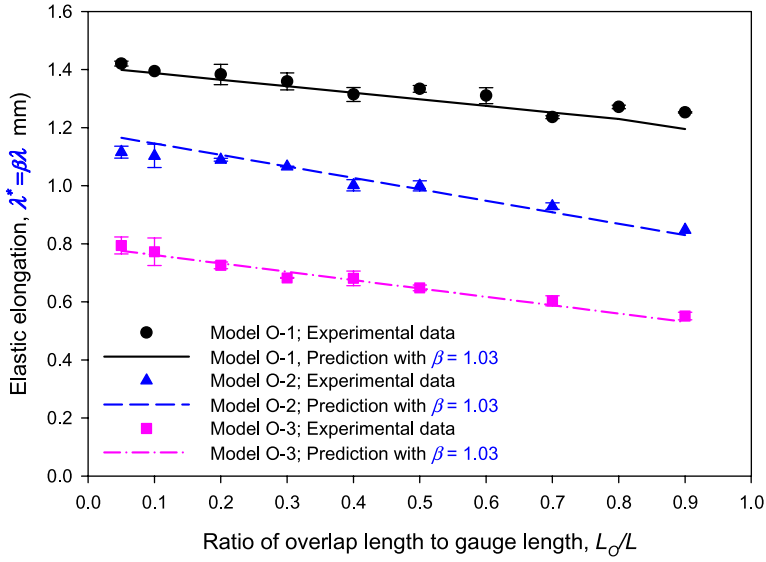

(a)

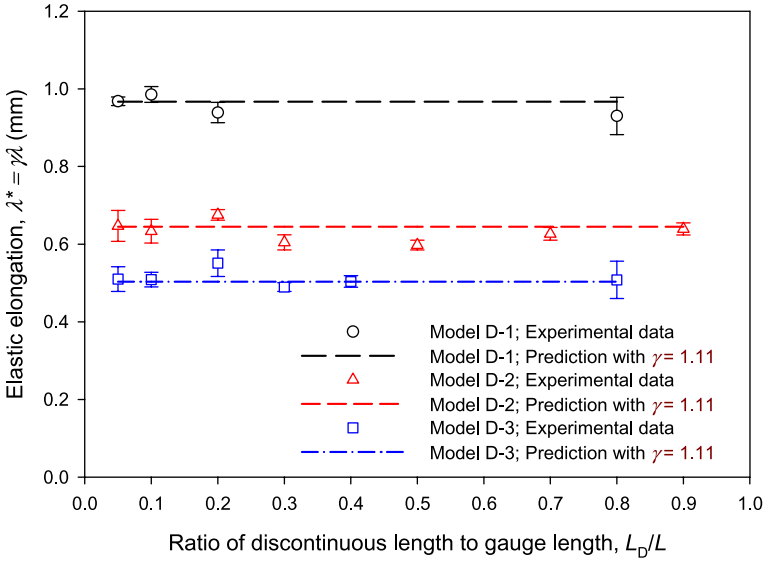

(b)

Figure 12. Experimental and predicted results of the elastic elongation: (a) overlaps (at $P = 2.01$ kN) and (b) discontinuities (at $P = 1.5$ kN). This figure is published in color in the online version.

a high modulus matrix (R235) when the effective fiber-volume fraction increased [21]. Using equation (9), the damage parameter regarding the tensile modulus of the K618/R409 composites due to the overlapped preform deformation could be predicted with $\beta = 1.04$, which was larger than the results for the K618/R235 composites. It can be inferred that for the overlapped preform deformation, the influence

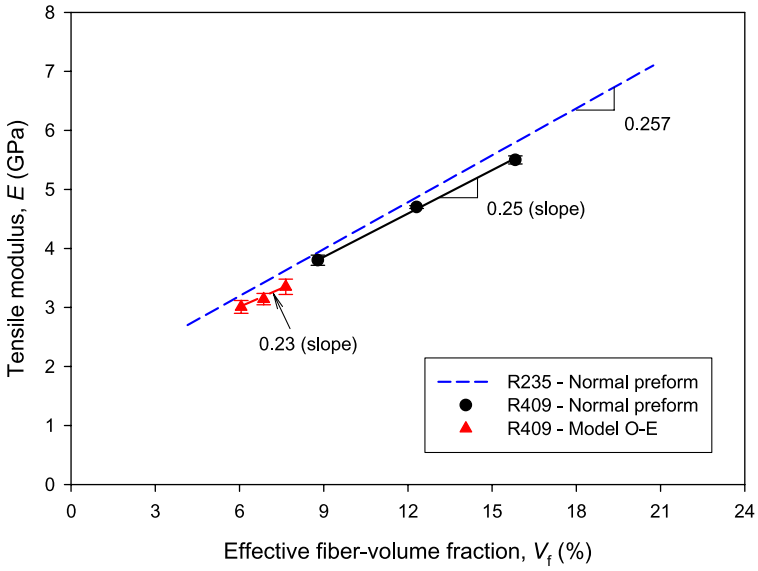

Figure 13. Variation of the tensile modulus with V_f for different matrices. This figure is published in color in the online version.

of composites with a low modulus matrix on the tensile modulus was larger than that of composites with a high modulus matrix.

4. Conclusions

The mechanical properties of composites that were fabricated from the normal, overlapped, and discontinuous fabric layers were examined and compared as functions of the effective fiber-volume fraction. This is necessary to enhance an understanding of the characteristics of the geometrical structure of the preform, and to design a composite wherein any resulting deformation, as in overlapped and discontinuous patterns, has only a slight influence on the mechanical properties in the respective composites.

The tensile strength of the overlapped and discontinuous models exhibits either one of two failure mechanisms, pulling failure and breaking failure, which depends on not only the materials but also the preform configuration. First, the failure type can be related to the tensile strength that is controlled by the interfacial bonding strength depending on the overlapped and discontinuous fabric lengths. Second, failure is controlled by the potential strength of the fabric when the overlapped and discontinuous lengths reached critical values.

As expected, the tensile modulus and strength increase with increasing fiber-volume fraction for any preform configuration. However, the curves of the properties of composites with a normal preform have steeper slopes compared to those under the overlapped and discontinuous models, which manifest degradation in load carrying and stress concentration. Also, those mechanical properties are more sen-

sitive to the discontinuous deformation than to the overlapped model. Generally, the overlapped and discontinuous patterns probably affect the quality of the finished composites, in terms of not only the tensile modulus and strength but also the elastic elongation as well as the failure mechanism. These influences are analyzed and described through the 'damage' parameters, which may relate to several factors such as the geometrical structure, materials, and processing and loading conditions.

Since discontinuous fabrics in the preform cannot be avoided for designing and manufacturing composites, the ratio of the discontinuous gap to the gauge length (L_G/L) should be less than 0.05. And the ratio of the discontinuous length to the gauge length (L_D/L) should be large to minimize the influence of the stress concentration. Also, the composites designed with the overlapped preform are better than those with the discontinuous preform as a function of the effective fiber-volume fraction.

Acknowledgement

This research was supported by a Research Grant from Yeungnam University in 2010.

References

1. K. F. Karlsson and B. T. Astrom, Manufacturing and applications of structural sandwich components, *Compos. A* **28**, 97–111 (1997).
2. T. Uozumi, A. Kito and T. Yamamoto, CFRP using braided preforms/RTM process for aircraft applications, *Adv. Compos. Mater.* **14**, 365–383 (2005).
3. C. Y. Chang, Modeling of filling process during resin injection/compression molding, *Adv. Compos. Mater.* **16**, 207–221 (2007).
4. H. Huang and R. Talreja, Effects of void geometry on elastic properties of unidirectional fiber reinforced composites, *Compos. Sci. Technol.* **65**, 1964–1981 (2005).
5. J. Varna, R. Joffe and L. A. Berglund, Effect of voids on failure mechanisms in RTM laminates, *Compos. Sci. Technol.* **53**, 241–249 (1995).
6. T. Czigany and K. Poloskei, Fracture and failure behavior of basalt fiber mat-reinforced vinylester/epoxy hybrid resins as a function of resin composition and fiber surface treatment, *J. Mater. Sci.* **40**, 5609–5618 (2005).
7. K. Potter, B. Khan, M. Wisnom, T. Bell and J. Stevens, Variability, fibre waviness and misalignment in the determination of the properties of composite materials and structures, *Compos. A* **39**, 1343–1354 (2008).
8. D. A. Steenkamer, D. J. Wilkins and V. M. Karbhari, The influence of preform joints on the processing of RTM composites, *Compos. Manuf.* **6**, 23–34 (1995).
9. A. R. Nalla, M. Fuqua, J. Glancey and B. Lelievre, A multi-segment injection line and real-time adaptive, model-based controller for vacuum assisted resin transfer molding, *Compos. A* **38**, 1058–1069 (2007).
10. J. A. Holmberg and L. A. Berglund, Manufacturing and performance of RTM U-beams, *Compos. A* **28**, 513–521 (1997).

11. F. Meraghni, C. J. Blakeman and M. L. Benzeggagh, Effect of interfacial decohesion on stiffness reduction in a random discontinuous-fibre composite containing matrix microcracks, *Compos. Sci. Technol.* **56**, 541–555 (1996).
12. J. L. Stanford, P. A. Lovell, C. Thongpin and R. J. Young, Experimental studies on the interfacial shear-transfer mechanism in discontinuous glass-fibre composites, *Compos. Sci. Technol.* **60**, 361–365 (2000).
13. Y. R. Zhao, Y. M. Xing, Z. K. Lei and F. C. Lang, Interfacial stress transfer behavior in a specially-shaped fiber/matrix pullout test, *Acta Mech. Sin.* **26**, 113–119 (2010).
14. J. Schuster and K. Friedrich, Modeling of the mechanical properties of discontinuous-aligned-fiber composites after thermoforming, *Compos. Sci. Technol.* **57**, 405–413 (1997).
15. H. K. Lee, S. H. Pyo and B. R. Kim, On joint strengths, peel stresses and failure modes in adhesively bonded double-trap and failure modes in adhesively bonded double-strap and supported single-lap GFRP joints, *Compos. Struct.* **87**, 44–54 (2009).
16. L. K. Jain and Y. W. Mai, Analysis of resin-transfer-moulded single-lap joints, *Compos. Sci. Technol.* **59**, 1513–1518 (1999).
17. P. K. Mallick, *Fiber-Reinforced Composites*. Marcel Dekker, New York, NY (1998).
18. R. M. Jones, *Mechanics of Composite Materials*. McGraw-Hill Kogakusha, Tokyo (1975).
19. T. T. Do and D. J. Lee, Effects of the wrinkled fabric preform on the bending properties of resin transfer molded composites, *J. Mater. Sci.* **44**, 4219–4227 (2009).
20. P. A. Sreekumar, K. Joseph, G. Unnikrishnan and S. Thomas, A comparative study on mechanical properties of sisal-leaf fibre-reinforced polyester composites prepared by resin transfer and compression molding techniques, *Compos. Sci. Technol.* **67**, 453–461 (2007).
21. Y. Arimitsu, S. Takahashi and T. W. Chou, Inter-fiber sliding in fabric shaping process, *Adv. Compos. Mater.* **12**, 23–34 (2003).
22. T. T. Do and D. J. Lee, Analysis of tensile properties for composites with wrinkled fabric, *J. Mech. Sci. Technol.* **24**, 471–479 (2010).
23. M. R. Piggott, *Load-Bearing Fibre Composites*. Pergamon Press, New York, NY (1980).
24. M. Bocciarelli, P. Columbi, G. Fava and C. Poggi, Fatigue performance of tensile steel members strengthened with CFRP plates, *Compos. Struct.* **87**, 334–343 (2009).
25. L. Tong and G. P. Steven, A numerical study on stresses in resin transfer moulding lap joints reinforced with transverse stitching, *Compos. Struct.* **36**, 91–100 (1996).
26. M. L. Costa, S. F. M. Almeida and M. C. Rezende, The influence of porosity on the interlaminar shear strength of carbon/epoxy and carbon/bismaleimide fabric laminates, *Compos. Sci. Technol.* **61**, 2101–2108 (2001).
27. T. Hobbiebrunken, M. Hojo, T. Adachi, C. D. Jong and B. Fiedler, Evaluation of interfacial strength in CF/epoxies using FEM and *in-situ* experiments, *Compos. A* **37**, 2248–2256 (2006).
28. A. Russo and B. Zuccarello, Experimental and numerical evaluation of the mechanical behaviour of GFRP sandwich panels, *Compos. Struct.* **81**, 575–586 (2007).
29. G. Kelly, Quasi-static strength and fatigue life of hybrid (bonded/bolted) composite single-lap joints, *Compos. Struct.* **72**, 119–129 (2006).
30. J. Moutier, M. Fois and C. Picard, Characterization of carbon/epoxy materials for structural repair of carbon/BMI structures, *Compos. B* **40**, 1–6 (2009).